

## Optical Centrifuge for Molecules

Joanna Karczmarek,<sup>1</sup> James Wright,<sup>2</sup> Paul Corkum,<sup>1</sup> and Misha Ivanov<sup>1</sup>

<sup>1</sup>*SIMS NRC, 100 Sussex Drive, Ottawa, Ontario, Canada K1A 0R6*

<sup>2</sup>*Ottawa-Carleton Chemistry Institute, Carleton University, Ottawa, Ontario, Canada K1S 5B6*

(Received 5 October 1998)

Strong infrared fields can be used for controlled spinning of molecules to very high angular momentum states. The angular momentum acquired can be sufficient to break molecular bonds. The approach is suitable for all anisotropic molecules, and we illustrate it by dissociating a homonuclear diatomic Cl<sub>2</sub>, with optical centrifuge efficiently separating Cl<sup>35</sup> and Cl<sup>37</sup> isotopes and thus demonstrating high sensitivity to the moment of inertia. [S0031-9007(99)09026-2]

PACS numbers: 33.80.Rv, 82.50.Fv

Optical manipulation of atoms (trapping, cooling, acceleration) has grown into a well-developed and established field. Its successful use of resonant processes is difficult to mimic for manipulation of molecules, due to the complexity of molecular energy spectra. However, intense nonresonant fields can provide forces similar to or even stronger than the resonant weak fields used in atom optics. Nonresonant forces have been long utilized in the manipulation of microscopic particles [1,2] but were only recently demonstrated for molecules, in optical deflection [3] and trapping [4] experiments. Molecular optics has a rich potential due to additional degrees of freedom offered by molecules. A range of molecular optics devices has been proposed [5] to control the external degrees of freedom using strong fields, while the field of coherent (or, more generally, active) control has been exploring ways to control the internal degrees of freedom [6]. We propose to use a nonresonant strong field to exert large optical torques on anisotropic molecules, leading to controlled molecular rotations induced with a simple pulse. This follows the work on strong field alignment [7] and complements the application of feedback control methods [8] to optimally excite specific angular momentum states. Molecular dissociation via rotations is used to demonstrate our method. The scheme distinguishes between molecules based on their moment of inertia, and thus acts as an optical centrifuge.

An anisotropic molecule placed in a linearly polarized infrared laser field experiences a time-averaged (over the laser cycle) potential  $-U_0 \cos^2 \theta$  due to the induced dipole moment interacting with the electric field. Here  $\theta$  is the angle between laser polarization and molecular axis, and  $U_0 = (1/4)(\alpha_{\parallel} - \alpha_{\perp})\mathcal{E}^2$ , with  $\mathcal{E}$  the field amplitude and  $\alpha_{\parallel}$  and  $\alpha_{\perp}$  the polarizability components parallel and perpendicular to the molecular axis [7]. Oblong molecules have  $\alpha_{\parallel} > \alpha_{\perp}$  and align with the electric field. For most diatomics,  $U_0 \sim 30\text{--}100$  meV can be achieved before ionization becomes important on the nanosecond time scale [3]. Imagine now slowly rotating the polarization of the infrared field about a fixed axis—the molecule will follow and rotate with

the same angular frequency. Accelerating the rotation of the polarization will increase the molecule's angular momentum in a controlled manner. This rotation results in large centrifugal forces which can distort or even break the molecular bonds, including those in homonuclear diatomics which do not readily absorb in the infrared.

The slowly rotating potential is produced by the field  $\vec{\mathcal{E}} = \mathcal{E}_0 \cos \omega t [\hat{x} \cos \phi_L(t) + \hat{y} \sin \phi_L(t)]$ . The time-dependent phase  $\phi_L(t)$  determines orientation of the polarization vector, which rotates in the  $xy$  plane with the frequency  $\Omega = \dot{\phi}_L$ . This field is a combination of two counterrotating circularly polarized beams:

$$\begin{aligned} \vec{\mathcal{E}} = & \frac{\mathcal{E}_0}{2} \{ \hat{x} \cos[\omega t + \phi_L(t)] + \hat{y} \sin[\omega t + \phi_L(t)] \} \\ & + \frac{\mathcal{E}_0}{2} \{ \hat{x} \cos[\omega t - \phi_L(t)] - \hat{y} \sin[\omega t - \phi_L(t)] \}. \end{aligned} \quad (1)$$

If the two beams are linearly chirped with respect to each other ( $\phi_L = \beta t^2/2$ ), the polarization rotates with constant acceleration  $\beta = \dot{\Omega} = \ddot{\phi}_L(t)$ , creating a steadily accelerating angular “trap” for the molecule. The two chirped fields can be obtained from a short (and hence broadband) laser pulse using a standard chirped pulse amplification technique; the maximum rotation frequency  $\Omega_{\max}$  is then limited by the pulse bandwidth  $\Delta\omega$ :  $\Omega_{\max} = \Delta\omega/2$ . Already for the light N<sub>2</sub> molecule a modest Ti:sapphire laser bandwidth of 35 nm yields a rotational energy  $I\Omega^2/2 \sim 1$  eV, where  $I$  is the moment of inertia. For heavier molecules  $I\Omega^2/2$  can easily approach their binding energy, stretching the bond to a point of breaking.

In Cartesian coordinates the Hamiltonian of this system is

$$H = \frac{1}{2\mu} \mathbf{p}^2 - \Omega(xp_y - yp_x) + V(R) - U_0(t, R) \frac{x^2}{R^2}. \quad (2)$$

Equation (2) is written in the frame rotating with the frequency  $\Omega = \beta t$  about the  $z$  axis, so that the electric field is fixed along the  $x$  axis.  $R = \sqrt{x^2 + y^2 + z^2}$  is the

internuclear distance,  $V(R)$  is the ground-state potential surface and  $U_0(R, t)$  is the depth of the laser-induced angular well which depends on time (following the intensity envelope) and on  $R$  (since the polarizability depends on  $R$ ), and  $\mu$  is the reduced mass. The Hamiltonian similar to Eq. (2) arises for a circular state of a Rydberg atom in a circularly polarized microwave field [9]. In such a system a nonspreading (“Trojan”) electronic wave packet can be forced to circulate about a positive ion core with a controlled angular frequency, following the rotation of the circularly polarized microwave field [9].

Before turning to numerical simulations, let us consider the case of constant  $U_0$  and look at a “quiet” trajectory starting with  $J = 0$ ,  $\theta \approx 0$  (aligned molecule), and negligible vibrational energy. While grasping the key features of the dissociation dynamics, as clear from comparing Figs. 1a and 1b ( $\tau \equiv 2B_e t = 2\pi$  is one ground-state rotational period), this trajectory permits significant simplification of the coupled three-dimensional problem.

The quiet trajectory stays in the  $xy$  plane, where its motion can be described in cylindrical coordinates by

$$\mu\ddot{R} = -\frac{\partial}{\partial R} \left( V(R) + \frac{J^2}{2\mu R^2} \right) \equiv -\frac{\partial}{\partial R} V_J(R), \quad (3)$$

$$\dot{J} = -U_0 \sin(2\theta) \approx -2U_0\theta, \quad (4)$$

where  $J = \mu R^2(\dot{\theta} + \Omega) = J_z$  and  $\Omega = \beta t$ . Qualitatively, the dynamics resembles that of a marble in a rotating spoon [with radial confinement due to  $V(R)$  and angular due to  $U_0(\theta)$ ]. As the rotation accelerates, the marble may fall off the spoon in radial direction (dissociation) or in tangential direction (loss from the  $\theta$  trap).

As long as the radial potential  $V_J(R)$  in Eq. (3) has a well, the quiet trajectory stays at its bottom, i.e.,  $R$  satisfies  $\mu\ddot{R} = -\partial V_J(R)/\partial R = 0$ . This yields an implicit dependence of  $R$  on the increasing  $J$  on the quiet trajectory,

$$J^2(R) = R^3 \mu \frac{\partial}{\partial R} V(R). \quad (5)$$

Equation (5) determines the position of the minimum of the radial well deformed by the centrifugal term. Figure 1a (inset) demonstrates excellent agreement between Eq. (5) and the numerical simulation of the quiet trajectory.

As  $J$  increases, the quiet trajectory defined by Eq. (5) follows the minimum of  $V_J(R)$  and moves to larger  $R$ . Dissociation occurs if  $J$  exceeds the threshold  $J = J_D$ , above which the radial potential  $V_J(R)$  has no well left. The obstacle to this arises from the Coriolis force: according to Eq. (4), changing  $J$  too quickly will cause  $\theta$  to increase. Going back to the marble-in-spoon analogy, the marble may roll off the side of the spoon before reaching its tip. This competition between the angular and the radial motions can be analyzed using Eqs. (4) and (5).

From the definition of  $J$  we have  $\dot{\theta} = -\Omega + J/\mu R^2(J)$ , where  $\Omega = \beta t$  and  $R(J)$  is obtained from Eq. (5). Differentiating Eq. (4), we obtain

$$\ddot{J} \approx -2U_0\dot{\theta} = 2U_0[\Omega(t) - J/\mu R^2(J)]. \quad (6)$$

As long as the equation  $\Omega(t) - J/\mu R^2(J) = 0$  has a solution  $J = J(\Omega(t))$ ,  $\ddot{J} = 0 = \dot{\theta}$ , and the angle  $\theta$  does not increase. Together with a steady increase of  $R(J)$  this describes the adiabatic stage of the quiet trajectory dynamics. This stage terminates before the dissociation threshold  $J_D$  is reached.

The inset of Fig. 1b shows that  $F(J) \equiv J/\mu R^2(J)$  reaches maximum at  $J = J_C$ . This means that as soon as  $\Omega = \beta t$  exceeds  $F_{\max} = J_C/\mu R^2(J_C)$ , the right-hand side of Eq. (6) can no longer be zero, and  $\ddot{J}$  becomes positive. This triggers the end of adiabatic evolution. For any potential  $V(R)$  with a single minimum  $J_C < J_D$  (see Fig. 1b, inset), thus adiabatic evolution is terminated before the dissociation threshold  $J_D$  is reached. As both  $\Omega = \beta t$  and  $J$  continue to increase [and  $F(J)$  decreases], the right-hand side of Eq. (6) grows quickly, triggering a fast increase of both  $\ddot{J}$  and  $-\dot{\theta}$ ; see Eq. (4). The molecule starts to lag behind the rotating angular trap.

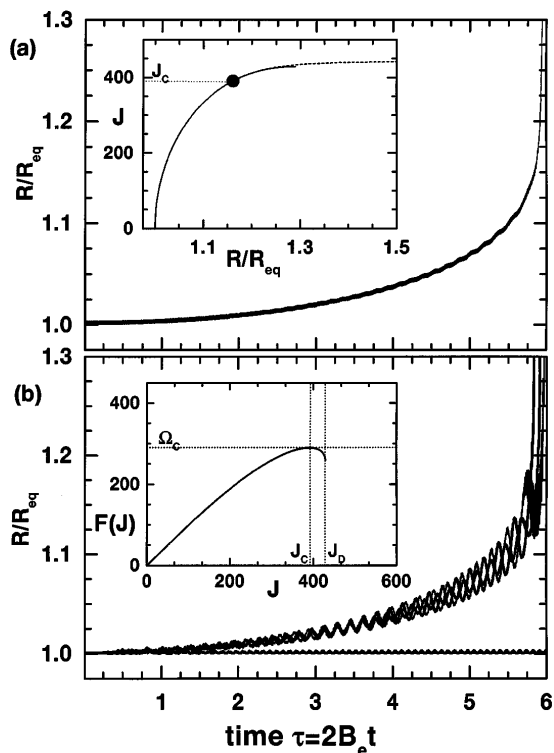


FIG. 1. Sample trajectories for  $\text{Cl}_2$ . The pulse is 70 ps long (equal to one ground rotational period of  $\text{Cl}_2$ , corresponding to  $\tau = 2\pi$  in our dimensionless units), with  $5.5 \text{ ps } \sin^2$  turn-on; the intensity is  $1.7 \times 10^{13} \text{ W/cm}^2$  [ $U_0(R_{\text{eq}}) = 56 \text{ meV}$ ];  $\Omega_{\text{final}} = 0.02 \text{ eV}$ . (a) The quiet trajectory; the inset shows agreement between the numerical calculation (dashed line) and Eq. (5) (solid line), and the dot represents  $J_C$  (see text). (b) Four sample trajectories  $R(t)$  for  $\text{Cl}_2$ . Initially,  $J = 30$  and a random orientation was chosen. Three trajectories show dissociation, and the fourth was not trapped. The inset shows  $F(J) \equiv J/\mu R^2(J)$  from Eq. (6).

Since  $J_C < J_D$ , the lag always starts before the bond is broken. Now we have a race: either  $J$  reaches  $J_D$  and the molecule dissociates or  $\theta$  exceeds  $\theta \sim -\pi/4$ , the molecule falls out of the  $\theta$  trap, and  $J$  plateaus at some value below  $J_D$ . For long bonds (e.g.,  $\text{Cl}_2$ ), where  $J_C$  is close to  $J_D$ , “ $J$  wins the race” and dissociation occurs. This is seen in Fig. 1a, inset: while the black dot corresponds to  $J = J_C$ , both  $R$  and  $J$  continue to increase beyond this point, for a while following the curve  $J(R)$  in Eq. (5). For short bonds (e.g.,  $\text{H}_2$ ) the molecule may be lost from the rotating well with some accrued  $J < J_D$ . The laser field, now rotating increasingly faster than the molecule, induces dynamics similar to that of a kicked rotor and may cause chaotic dissociation.

To achieve rotational excitation, we must successfully confine molecules to the angular well during the field turn-on. This restricts the turn-on  $t_{\text{on}}$  to

$$\sqrt{\frac{2\pi}{\beta}} < t_{\text{on}} < \sqrt{\frac{U_0}{I\beta^2}}. \quad (7)$$

Indeed, with the instantaneous turn-on it is impossible to trap molecules for some initial orientations. Sweeping out an angle of at least  $\pi$  while switching on the angular trap ( $\beta t_{\text{on}}^2/2 > \pi$ ) relieves this problem for rotationally cold molecules; this is the lower bound in Eq. (7). For a rotationally cold molecule in the  $xy$  plane, the kinetic energy accumulated during the turn-on is  $K \sim U_0/2 + I(\beta t_{\text{on}})^2/2$ . Here  $U_0/2$  comes from the virial theorem, and  $I(\beta t_{\text{on}})^2/2$  is due to the rotation of the frame. The molecule is trapped if  $K < U_0$ , placing an upper bound on  $t_{\text{on}}$ . Our numerical simulations in two dimensions show that the number of trapped molecules which were initially moving in the  $xy$  plane decreases sharply as  $t_{\text{on}}$  is extended beyond the upper limit in Eq. (7). In three dimensions this decrease is slower, since a molecule can become trapped even if  $K > U_0$ , provided it is moving in the right direction.

Equation (7) limits the maximum chirp,  $I\beta < U_0/(2\pi)$ . This also guarantees that the angular acceleration of the rotating trap  $\beta$  does not exceed the characteristic angular acceleration  $\epsilon$  that the trapping potential  $-U_0 \cos^2\theta$  can apply to a molecule,  $I\epsilon \sim U_0/\pi$ . The same inequality  $2\pi I\beta < U_0$  gives a condition on a minimum pulse energy per area in a form  $U_0 T_{\text{pulse}} > 2\pi I\Omega_{\text{final}}$  (see also note [10]).  $\Omega_{\text{final}}$  is fixed either by how fast we want to spin the molecule, or by the bandwidth of the laser.

We have used  $\text{Cl}_2$  as an example for numerical computations with the Hamiltonian in Eq. (2).  $V(R)$  was generated using a multireference configuration interaction approach [11] with a basis set of  $10s7p2d$  contracted Gaussian functions on each Cl atom and additional ( $s, p$ ) functions midway between the nuclei. The most important configurations were selected based on their ability to lower the total energy by interaction with a set of four reference configurations, leading to Cl spaces of dimension

ca. 10000. The static polarizabilities  $\alpha_{\parallel,\perp}$  were calculated using the GAUSSIAN94 program [12] with method/basis MP2/6-311 + +G(3df). Sample trajectories for a simple laser pulse (see caption) and  $J = 30$  (typical value at a room temperature) are shown in Fig. 1. Three of the trajectories in Fig. 1b correspond to molecules which spun and dissociated, while the fourth did not become rotationally trapped.

Figure 2 shows initial and final distributions of  $J_z$  for two fixed initial  $J$ 's and the same laser pulse. The initial conditions correspond to a microcanonical ensemble for the given  $J$  and a ground vibrational state. The high- $J_z$  peak corresponds to dissociated molecules (the simulation was halted at  $R = 10R_{\text{eq}}$ ). The low- $J_z$  peak represents molecules which were not rotationally trapped. All rotationally trapped trajectories dissociated, yielding fragments with kinetic energy  $\sim 1.1$  eV. Notice high efficiency of dissociation even for initial  $J = 30$  (typical at room temperature).

Larger moment of inertia means that smaller bandwidth is required to attain the same rotational energy  $\frac{1}{2}I\Omega_{\text{final}}^2$ . This can be used, for example, to separate isotopes (the heavier species will dissociate first). We illustrate this with the three types of  $\text{Cl}_2$  molecule: 35-35 (57%), 35-37 (37%), and 37-37 (6%). Figure 3 shows the distribution of “breaking times” [defined here as the time when  $R(t) = 2R_{\text{eq}}$ ] for each of the three molecules, initially rotationally cold; the pulse is the same as in Figs. 1 and 2. If the pulse ends at the time indicated by the vertical line, with a 100 fs turn-off, our simulation shows that 8.5% of  $\text{Cl}_2$  37-37 is broken, with only 0.6% of  $\text{Cl}_2$  35-37 and none of the  $\text{Cl}_2$  35-35 (12 800 trajectories were used for each molecule). Thus, the ratio of  $\text{Cl}^{37}$  to  $\text{Cl}^{35}$  in the “debris” is 5.6:1, starting with the natural abundance of 1:3.

Vibrationally excited diatomics dissociate at smaller angular momenta  $J$ , as soon as the vibrational state is not bound by the potential  $V_f(R)$ , Eq. (3). For example, in our simulations  $\text{Cl}_2$  vibrationally excited by one-third

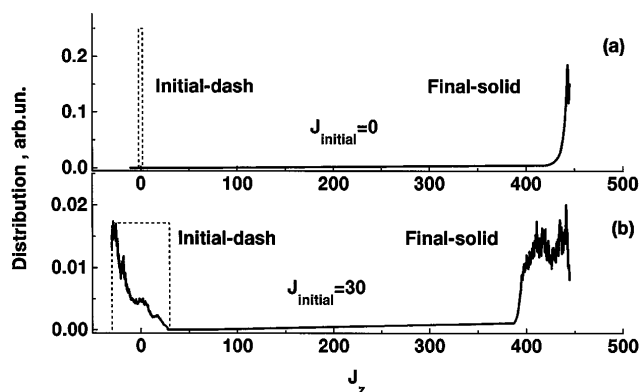


FIG. 2. Rotational dissociation of  $\text{Cl}_2$ . Pulse parameters are the same as in Fig. 1a. (a)  $J_{\text{initial}} = 0$ , 12 813 trajectories; (b)  $J_{\text{initial}} = 30$  (thermal peak at  $T = 300$  K), 41 920 trajectories.

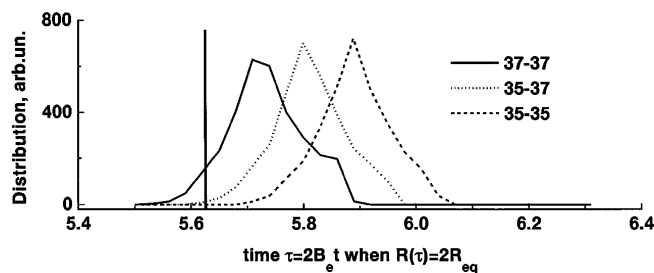


FIG. 3. Isotope separation for rotationally cold  $\text{Cl}_2$ . The pulse is the same as in Figs. 1 and 2. Probability distribution for time at which  $R = 2R_{\text{eq}}$  is shown; 3200 trajectories were used for each plot.

of the binding energy dissociated at 80% of  $\Omega_{\text{final}}$  required for  $\text{Cl}_2$  in its ground state. This should allow for successive “peeling off” of the vibrational states, as is done with a dc field for Rydberg atoms.

The optical centrifuge can be used to selectively dissociate a given diatomic from a mixture. In a mixture of  $\text{Cl}_2$  and  $\text{I}_2$  one can easily dissociate the heavier [ $I(\text{I}_2) : I(\text{Cl}_2) = 13 : 2$ ] and weaker bound (by 40%)  $\text{I}_2$  without breaking  $\text{Cl}_2$ . Larger centrifugal forces may preferentially break the heavier molecule even if it is stronger bound. We can also choose to selectively spin and hence break the lighter (and stronger bound)  $\text{Cl}_2$  by tailoring  $t_{\text{on}}$ , using the upper bound in Eq. (7). Choosing  $\sqrt{U_0/I\beta^2}|_{\text{I}_2} < t_{\text{on}} \approx \sqrt{U_0/I\beta^2}|_{\text{Cl}_2}$  will ensure efficient trapping of chlorine with inefficient trapping of iodine.

Our scheme is analogous to the (linear) acceleration of cold atoms in a moving optical lattice created by slightly detuned counterpropagating linearly polarized waves [13]. Acceleration-induced tunneling between the wells of such a lattice [13] has a direct analog in our case; however, it is not important on our picosecond time scale.

Our method of using two chirped circular fields for rotational excitation (rotational ladder climbing) complements the proposal [14,15] to use a chirped linearly polarized field for vibrational ladder climbing. While rotations are a nuisance in the scheme of Refs. [14,15], we use them to our advantage.

In Ref. [15], classical calculations of vibrational ladder climbing were shown to be sufficient for heavy atoms such as Cl and an elegant quantum-classical correspondence was uncovered there. Classical calculations should also be sufficient for our purposes. The classical-quantum correspondence here is both deep and clear. Quantum mechanically, rotational excitation in the field Eq. (1) arises from Raman transitions  $|J - 1, J_z - 1\rangle \leftrightarrow |J + 1, J_z + 1\rangle$ , where  $\omega + \Omega$  photon is absorbed and  $\omega - \Omega$  photon is emitted. The resonance condition is  $2\Omega = E_{J+1} - E_{J-1}$ . For  $J \gg 1$  the energy difference is  $E_{J+1} - E_{J-1} \approx 2J/\mu R^2(J)$ , where  $R(J)$  is the equilibrium position of the binding potential  $V(R)$ , modified by the centrifugal term  $J^2/2\mu R^2$  [see Eq. (5)]. Thus, the resonance condition reads  $\Omega(t) = J/\mu R^2(J)$ . This con-

dition is familiar from the right-hand side of the classical Eq. (6), where it allows for an adiabatic increase of  $J$  on the quiet trajectory, following the acceleration of the angular trap. This resonance condition could also be used to optimize the chirp once the bond is so strongly distorted that  $E_{J+1} - E_{J-1} \approx 2J/\mu R^2(J) = 2F(J)$  starts to decrease (at  $J > J_C$ ).

In the future, it appears attractive to investigate the application of this technique to larger molecules such as  $\text{H-C}\equiv\text{N}$ , with a strong bond between the heavier atoms. Since H is light compared to C and N, the centrifugal force exerted on the triple bond should be significantly greater (by a factor of  $\sim 6$ ) than that exerted on the single bond. The role of the Coriolis coupling in this case requires further study.

We gratefully acknowledge fruitful discussions with P. Bucksbaum, A. Stolow, T. Fortier, G. DiLabio, D. Matusek, K. Rzazewski, I. Bialynicki-Birula, and B. Friedrich. We thank P. Bellomo for suggesting the “marble-in-the-spoon” analogy.

- [1] A. Ashkin, J.N. Dziedzic, J.E. Bjorkholm, and S. Chu, *Opt. Lett.* **11**, 288 (1986).
- [2] M.E.J. Friese *et al.*, *Nature (London)* **394**, 348 (1998).
- [3] H. Stapefeldt *et al.*, *Phys. Rev. Lett.* **79**, 2787 (1997).
- [4] T. Takekoshi, B.M. Patterson, and R.J. Knize, *Phys. Rev. Lett.* **81**, 5105 (1998).
- [5] T. Seideman, *J. Chem. Phys.* **106**, 2881 (1997); H. Sakai *et al.*, *Phys. Rev. A* **57**, 2794 (1998).
- [6] R.J. Gordon and S.A. Rice, *Annu. Rev. Phys. Chem.* **48**, 601 (1997); M. Shapiro and P. Brumer, *J. Chem. Soc. Faraday Trans.* **93**, 1263 (1997).
- [7] B. Zon and B. Katsnelson, *Zh. Eksp. Teor. Fiz.* **69**, 1166 (1975) [*Sov. Phys. JETP* **42**, 595 (1976)]; B. Friedrich and D. Herschbach, *Phys. Rev. Lett.* **74**, 4623 (1995).
- [8] H. Rabitz, *Adv. Chem. Phys.* **101**, 315 (1997); R.S. Judson and H. Rabitz, *Phys. Rev. Lett.* **68**, 1500 (1992).
- [9] M. Kalinski and J.H. Eberly, *Opt. Expr.* **1**, 215 (1997); I. Bialynicki-Birula, M. Kalinski, and J.H. Eberly, *Phys. Rev. Lett.* **73**, 1777 (1994); I. Bialynicki-Birula and Z. Bialynicka-Birula, *Phys. Rev. Lett.* **77**, 4298 (1996); A.F. Brunello, T. Uzer, and D. Farrelly, *Phys. Rev. Lett.* **76**, 2874 (1996).
- [10] This also means  $D_e \gg I\beta$  ( $D_e$  the dissociation energy), which ensures negligible coupling of rotations to the electronic degree of freedom—B. Friedrich (private communication).
- [11] R.J. Buenker and R.A. Phillips, *J. Mol. Struct. Theochem.* **123**, 291 (1985).
- [12] M.J. Frisch *et al.*, *Gaussian 94 rev. B.3* Gaussian Inc., Pittsburgh, PA, 1994.
- [13] Q. Niu and M.G. Raizen, *Phys. Rev. Lett.* **80**, 3491 (1998).
- [14] S. Chelkowski, A.D. Bandrauk, and P.B. Corkum, *Phys. Rev. Lett.* **65**, 2355 (1990); S. Chelkowski and A.D. Bandrauk, *J. Chem. Phys.* **99**, 4279 (1993).
- [15] W.-K. Liu, B. Wu, and J.-M. Yuan, *Phys. Rev. Lett.* **75**, 1292 (1995).